

Correlation between epithelial thickness in normal corneas, untreated ectatic corneas, and ectatic corneas previously treated with CXL; is overall epithelial thickness a very early ectasia prognostic factor?

Anastasios John Kanellopoulos^{1,2}
Ioannis M Aslanides³
George Asimellis¹

¹Laservision Eye Institute, Athens,
²Emmetropia Mediterranean Eye Clinic, Crete, Greece, ³New York University School of Medicine, NY, USA

→ Video abstract



Point your SmartPhone at the code above. If you have a QR code reader the video abstract will appear. Or use: <http://dx.doi.org/10.2147/OPHTH.S31524>

Correspondence: A John Kanellopoulos
Laservision Eye Institute, 17A Tsocha str,
Athens, Greece 11521
Tel +30 210 747 2777
Fax +30 210 747 2789
Email ajk@brilliantvision.com

Purpose: To determine and correlate epithelial corneal thickness (pachymetric) measurements taken with a digital arc scanning very high frequency ultrasound biomicroscopy (HF UBM) imaging system (Artemis-II), and compare mean and central epithelial thickness among normal eyes, untreated keratoconic eyes, and keratoconic eyes previously treated with collagen crosslinking (CXL).

Methods: Epithelial pachymetry measurements (topographic mapping) were conducted on 100 subjects via HF UBM. Three groups of patients were included: patients with normal eyes (controls), patients with untreated keratoconic eyes, and patients with keratoconic eyes treated with CXL. Central, mean, and peripheral corneal epithelial thickness was examined for each group, and a statistical study was conducted.

Results: Mean, central, and peripheral corneal epithelial thickness was compared between the three groups of patients. Epithelium thickness varied substantially in the keratoconic group, and in some cases there was a difference of up to 20 μm between various points of the same eye, and often a thinner epithelium coincided with a thinner cornea. However, on average, data from the keratoconic group suggested an overall thickening of the epithelium, particularly over the pupil center of the order of +3 μm , while the mean epithelium thickness was on average +1.1 μm , compared to the control population ($P = 0.005$). This overall thickening was more pronounced in younger patients in the keratoconic group. Keratoconic eyes previously treated with CXL showed, on average, virtually the same average epithelium thickness (mean $-0.7 \mu\text{m}$, $-0.2 \mu\text{m}$ over the pupil center, $-0.9 \mu\text{m}$ over the peripheral zone) as the control group. This finding further reinforces our novel theory of the “reactive” component of epithelial thickening in corneas that are biomechanically unstable, becoming stable when biomechanical rigidity is accomplished despite persistence of cornea topographic irregularity.

Conclusion: A highly irregular epithelium may be suggestive of an ectatic cornea. Our results indicate that the epithelium is thinner over the keratoconic protrusion, but to a much lesser extent than anticipated, and on average epithelium is thicker in this group of patients. This difference appears to be clinically significant and may become a screening tool for eyes suspected for ectasia.

Keywords: corneal pachymetry, ectasia, keratoconus screening, cornea epithelial thickness

Introduction

Importance of corneal epithelium imaging

The contribution of the corneal epithelium to the refractive power of the cornea, and thus ocular refraction, cannot be ignored. Studies have shown that epithelial refractive

power alone is an average of 1.03 D (range 0.55–1.85 D) over the central 2 mm diameter zone¹ and 0.85 D (range 0.29–1.60 D) at the 3.6 mm diameter zone.¹

Knowledge of the specific epithelium thickness distribution may prove beneficial in close call clinical judgments and aid in the safe screening of a candidate for excimer-laser corneal refractive surgery. The reason for this is that the epithelium does not have homogeneous depth (mean $53.4 \pm 4.6 \mu\text{m}$) over the Bowman's layer.² The epithelium tends to compensate for stromal surface irregularities, ie, by being thicker over the “valleys” and thinner over the “hills”, where the stroma protrudes. Central epithelial thickness in normal eyes has been reported to be thicker than those of keratoconic eyes (mean difference $+2.1 \mu\text{m}$), and the epithelium is thinner superiorly than inferiorly in normal eyes (mean difference $-1.4 \mu\text{m}$).² It has been therefore suggested that the epithelium attempts to minimize abrupt changes in stromal thickness. As a result, the cornea may project a smoother topography and an alleviated wavefront error map, compared to what the underlying anterior stroma alone would show.

In the specific case of subclinical corneal ectasia, if the epithelium is thinner over the ectatic area, profile maps may help a clinician who would otherwise be reading a total corneal pachymetry map to identify patients in whom corneal ablative procedures are contraindicated.³ However, if the epithelium is thicker centrally, an assessment based only on total corneal pachymetry – topography, with no knowledge of the specific epithelial depth – may result in an incorrect assessment of keratoconic progression.

Epithelium thickness irregularities can also be detected in contact lens wearers, who are likely to exhibit epithelium wrapping^{4,5} or arcuate lesions,⁶ thus leading to incorrect assessment of their true refraction. Epithelium properties have also been investigated in eyes of patients with diabetes mellitus.^{7,8} In addition, a large number of refractive errors after laser refractive cornea surgery such as LASIK may be explained by epithelial factors.

For the reasons described above, devices providing precise and accurate in vivo measurements of epithelial thickness distribution over the entire cornea are very important.

Optical-based anterior segment imaging technologies

While the most advanced and established corneal imaging systems are mainly optical, they cannot provide visualization of epithelial thickness, ie, they cannot discern epithelial from stromal components within the cornea because corneal layers

have minimal refractive index changes in order to prevent internal reflections.

The two exceptions are anterior segment optical coherence tomography (AS OCT)^{9–11} and confocal microscopy.^{12,13} To a lesser degree, optical pachymetry¹⁴ and through focusing confocal microscopy¹⁵ are also capable of discerning epithelium. All these methods, however, are limited to specific points, ie, spot measurements or a single meridian B-scan of the cornea, thus are not suitable for providing a full area visualization of the epithelial thickness map.

Spectral domain (SD) OCT¹⁶ signal processing employs Fourier transformation of the optical spectrum of a low coherence interferometer, enabling excellent axial resolution (how close together along the direction of beam propagation two points can be distinguishable from each other) down to $5 \mu\text{m}$. Lateral (or transverse) resolution (ability to distinguish two points located normal to each other along the direction of propagation) is limited by ocular optics, the numerical aperture of the illuminating beam, and the number of A-scans employed in the construction of the B-scan.

Currently, there are a number of SD OCT systems commercially available with anterior segment imaging capabilities. These include the Visante (Carl Zeiss Meditec AG, Jena, Germany), Optovue RTVue (Optovue Inc, Fremont, CA), OCT/SLO Combination Imaging System (Optos Inc, Marlborough, MA), and SS-1000 CASIA (Tomey Corporation, Nishi-Ku, Nagoya, Japan).¹⁷

The high resolution and precision offered by these systems enables local visualization and segmentation of anterior corneal and epithelial boundaries in a specific meridional scan. Typically, such systems provide corneal pachymetric maps, as well as high resolution cross-sectional images across a meridian of choice. In many of these systems, meridional scan images can be used to calculate epithelial thickness via the caliper tool.^{18,19} However, to produce epithelial topography (thickness profile) continuously over an area covering the entire cornea, dedicated software to interpolate thickness profile calculated from each meridian is required.²⁰ To the best of our knowledge, this is not offered commercially for any clinical imaging system.

Ultrasound-based anterior segment imaging technologies

Real-time in vivo epithelial mapping is possible with high frequency ultrasound biomicroscopy (HF UBM) systems.^{21–23} The major advantage of ultrasound over optically based systems is that they are not hindered by optically opaque intervening ocular structures. Ultrasound systems, however,

require fluid coupling to the eye, and thus necessitate more effort by the examiner and a higher degree of compliance from the patient.

The inception of technology for use in ocular imaging dates back to the 1950s with the work of Mundt and Hughes²⁴ (A-scan) and Baum and Greenwood²⁵ (B-scan). A-scan systems are mainly contact (and thus require local corneal anesthesia), whereas B-scan systems involve scanning. The latter are advantageous over the former, which suffer from variability largely related to decentration, oblique incidence which may cause spuriously thicker measurements, possible corneal compression by the probe, and risk of epithelium scarring, corneal injury, and infection. B-scans require mechanical scanning of the acoustic transducer and setting pixel intensity in proportion to echo amplitude along each line of sight. However, for many years the axial resolution of these systems had been limited because the center frequency had been restricted to the vicinity of 10 MHz.

The evolution of conventional B-scanning, termed UBM, appeared much later.²⁶ Coupled with the introduction of high frequencies in the range of 35–50 MHz, as well as improvements in scanning, data processing, and display, UBM enabled substantial improvements in both axial and lateral resolution down to 40 μm or less. The first UBM system which allowed meaningful clinical application of corneal imaging was developed by Foster and colleagues in the early 1990s, resulting in the ultrasound biomicroscope manufactured by Zeiss-Humphrey Instruments (San Leandro, CA).²⁷ Almost simultaneously, Silverman and colleagues independently developed a digital UBM arc scanner system emphasizing the processing of raw echo data in a non-contact immersion method.²¹ This system was eventually commercialized as the Artemis, which has received United States Food and Drug Administration approval and is commercially available.

The Artemis system uses a lithium niobate transducer operating on a broad band 50 MHz very high frequency. The cornea is offset from the probe as the patient places the eye over a disposable soft rimmed eye cup, and the area is then filled by sterile normal saline solution at

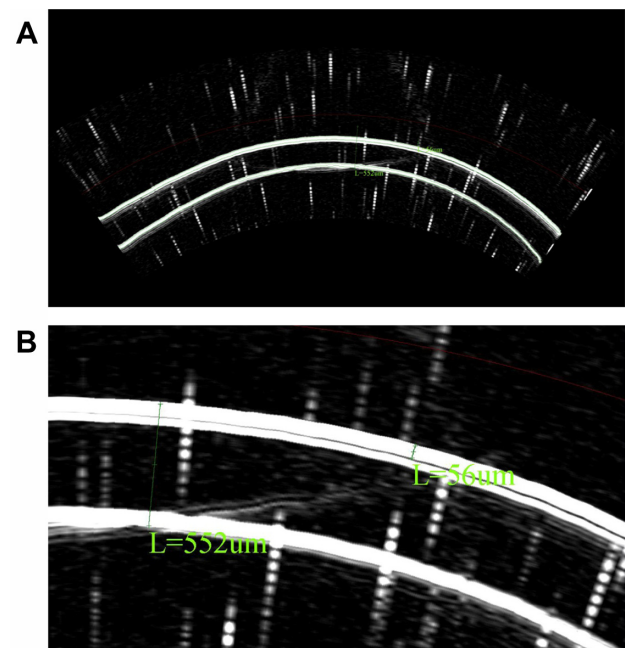


Figure 1 B-scan reconstruction, as obtained from the HF UBM system showing epithelium and corneal thickness measurements via the caliper tool. We observe the anterior and posterior cornea, as well as the cornea–epithelium interface. (A) Full scan, scale 8.4 $\mu\text{m}/\text{pixel}$. (B) Detail.

room temperature. The ultrasound transducer and scan mechanism are submerged in deionized water (27°C–33°C) within the body of the scanner and separated from the eye by the transparent membrane provided by the disposable eye cup. In the raw data (A-scans) the local maxima correspond to the interfaces where there is a localized change of impedance, such as the epithelium–immersion water, Bowman’s interface–anterior stroma, and inferior stroma (including Descemet’s membrane)–aqueous humor. The system claims resolution of 21 μm , whereas the precision of measurement varies according to position within the cornea, with 0.5 μm at the center and less than 1.3 μm peripherally.²⁸ Examples of B-scan images obtained via the Artemis II are presented in Figure 1.

Visualization of epithelium mapping can be quite valuable in the decision making process as well as in the short- and long-term postoperative assessment of excimer-laser corneal refractive surgery procedures. It is also valuable

Table 1 Age characteristics of patients

Group	Age (years)				Patients (n)	Eyes tested (n)
	Average	SD	Min	Max		
Control	32.4	12.7	16	68	33	50
KCN – not treated	28.4	6.8	16	45	26	39
KCN – CXL treated	29.2	9.4	16	72	42	70

Abbreviations: CXL, crosslinking; KCN, keratoconus; SD, standard deviation.

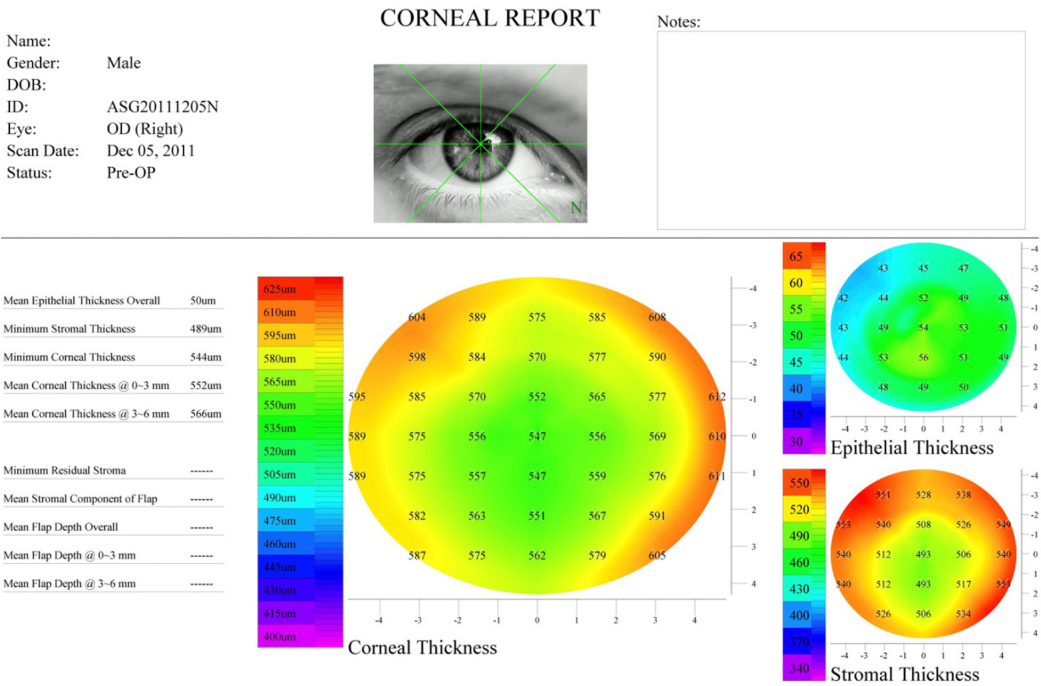


Figure 2 Corneal report produced by the Zeus software showing total corneal, epithelial, and stromal thickness pachymetry maps over 8 mm diameter. **Notes:** The subject's eye is normal. We observe the overall thicker epithelium over the pupil center.

in the assessment of crosslinking (CXL) postoperative epithelial healing, and keratoconus (KCN) and pellucid marginal degeneration screening. Despite its large potential, epithelium mapping is underreported amongst researchers and underused as a diagnostic tool by clinicians, compared to total corneal pachymetry (eg, mapping the whole cornea). This is because current optically-based corneal imaging systems have limited capability to discern epithelial from stromal components within the cornea over the entire corneal area.

The scope of our work is to explore the efficacy of a high frequency arc scanning UBM system, namely the Artemis II + superior (Artemis Medical Technologies Inc, Vancouver, British Columbia, Canada) in the task of clinical epithelial corneal mapping in normal corneas, and keratoconic corneas either nontreated or treated with collagen CXL.

Materials and methods

Epithelial evaluation via 3-D mapping (surface pachymetric measurements) was conducted with the Artemis II + superior. This study was approved by the Ethics Committee. Informed consent for all testing was obtained from each volunteer. To screen for ocular abnormalities each patient underwent a complete ocular examination, including manifest refraction, autorefraction and keratometry measurements. (Auto Refkeratometer Speedy-K Nikon Ophthalmic Instruments Miyagi, Japan), and tomography (Pentacam HR, Oculus Optikgerate GmbH, Wetzlar, Germany). This study included three groups of patients: those with normal eyes who served as controls (n = 33), patients with untreated keratoconus (n = 26), and patients with keratoconus treated at least 6 months prior to diagnosis with CXL and simultaneous partial, topography-guided photoreactive keratectomy (n = 42) (Table 1). Normal

Table 2 Mean central corneal and epithelium thickness, as measured by HF UBM for the same patient and the same eye, as a result of different meridian selections acquired during a single examination session

	CCT	Thickness (μm)					
		CET	%	N	T	S	I
Mean (μm)	542.72	50.92	9.38	50.77	46.96	46.55	48.99
SD (μm)	3.71	3.22	0.56	2.53	3.69	3.04	3.30
% SD	0.7%	6.3%	6.0%	5.0%	7.9%	6.5%	6.7%
Confidence interval (95%)	542.40 to 543.03	50.65 to 51.19		50.55 to 50.98	46.64 to 47.27	46.30 to 46.81	48.71 to 49.27

Abbreviations: CCT, central corneal thickness; CET, central epithelial thickness; HF UBM, high frequency ultrasound biomicroscopy; I, inferior; N, nasal; %, percentage of CET over CCT; S, superior; SD, standard deviation; T, temporal.

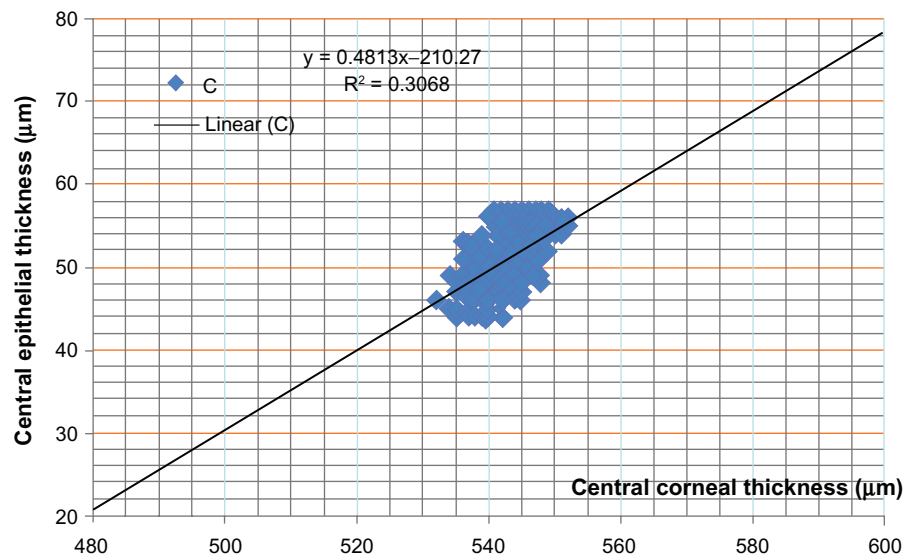


Figure 3 Central epithelial thickness versus central corneal thickness of the same data points as produced by 540 different combinations of select meridional scans.
Note: All data correspond to the same eye.

eyes were defined as eyes with corneas that did not have any ectasia criteria, based on cornea tomographic measurements, and noted as normal on the keratoconus screening software available on the Pentacam HR. Keratoconic eyes were defined as eyes diagnosed with keratoconus based on the same criteria. The

average postoperative time elapsed for the group of CXL ectatic eyes was 28.9 ± 12.4 months (range 6 months to 6 years).

HF UBM measurements

Ultrasound imaging data were stored and processed via the Zeus V 1.0 (Build 11.780) software, licensed from Artemis Medical Technologies, Inc. The software assumes a constant speed of sound of 1640 m/s throughout the ocular media. From each eye, the scan sequence consisted of four meridional B-scans at 45° intervals, namely horizontal, 45°, vertical, and 135°. Each scan sweep took about 0.25 seconds and consisted of 256 scan lines (pulse echo vectors). During the acquisition of each scan, raw data were converted (in near real time) to a B-scan displayed on the computer screen. Each B-scan reveals information regarding centration, ranging, and eye movements that may have occurred during the scan sweep. The examiner either accepted or chose to repeat a particular meridional sweep before proceeding to the next. At least three full scans per meridian were stored. The digitized ultrasound data were then transformed via Zeus software, which includes auto-correlation of back surface curvatures to center and aligns the meridional scans.

During acquisition, the center of rotation of the system was adjusted until it was coaxial with the corneal center, as seen from the internal camera. Following fixation and centering, total acquisition time was in the order of a few minutes. Of the two options offered, we selected the corneal analysis to be “centered on the middle of the scan”, and we did not select “circle-filter to smooth the map”.

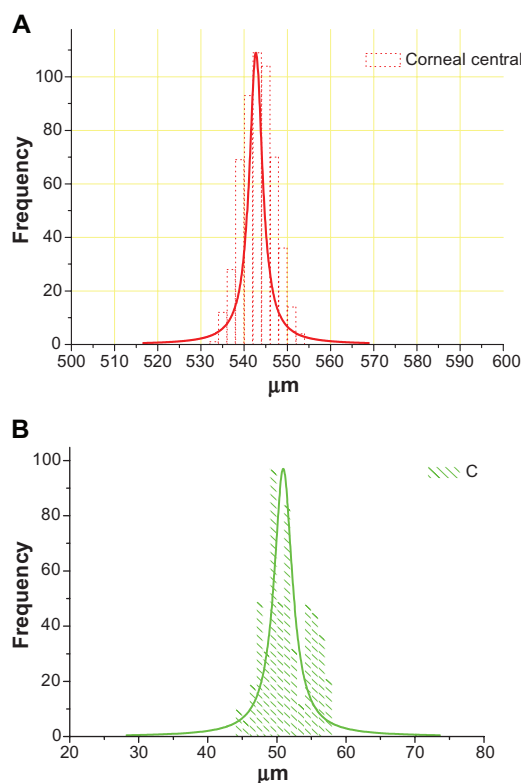


Figure 4 Central corneal (A) and central epithelial (B) thickness histogram plots of the same data points as produced by 540 different combinations of select meridional scans.
Note: All data correspond to the same eye.

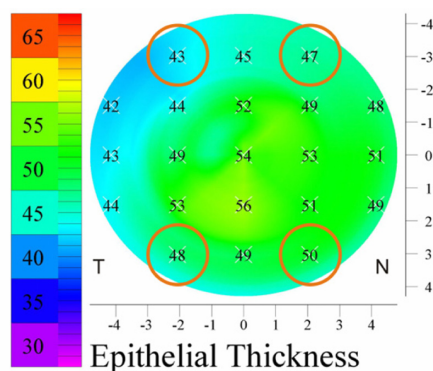


Figure 5 The four transitional zone points used to calculate peripheral epithelium thickness on each eye.
Note: Epithelium thickness from these points was averaged, and is referred to as peripheral epithelium thickness.

From the group of stored scans, the examiner selected one scan (the most representative, most complete and centered acquisition) from each meridian to be included in the thickness profile report. A linear polar/radial interpolation function was used to interpolate among the selected scans to produce an 8 mm diameter map.

Descriptive statistics, comparative statistics, and linear regression were performed via Microsoft Excel 2010 (Microsoft Corp, Redmond, WA) and Origin Lab version 8 (OriginLab Corp, Northampton, MA). Statistical analysis was performed via the Origin Lab and IBM SPSS statistics tool (v.19.0).

Results

Precision dependence on meridional scan selection

One of the first issues to be investigated was the influence of meridional scan selection and number of acquisition scans on the precision of produced thickness measurements. As stated above, the same examiner selected the most representative scan to be included in the report. Currently the software does not offer the option of averaging of a number of same-meridian scans. We wanted to investigate how the selection among apparently equally well-suited choices of

scans (for the same meridian) affects the precision of the reported values.

For this reason one male participant (normal eye) was subjected to a more extensive study, and a total of 20 meridional scans (ie, five scans per meridian) were stored. All possible different combinations of scan selections were considered to produce corneal pachymetry reports as shown in Figure 2. Results from all possible combinations (n = 540) were subsequently tabulated and statistically analyzed (Table 2).

Figure 3 demonstrates the correlation between central corneal thickness versus central epithelial thickness for the same point corresponding to the same data whose descriptive statistics appear in Table 2. Figure 4 shows the histogram graphs for central corneal thickness and central epithelial thickness for the same eye, as produced by the 540 different meridional combinations.

Data validation and collection

Our study of epithelial thickness maps was based on the concept of data validation. Of the 33 control group patients, 11 were female and 22 were male. Of the 26 untreated keratoconic patients, 7 were female and 19 were male. Of the 42 CXL-treated patients, 13 were female and 29 were male. For some patients, eyes were categorized into different groups (if, for example only one eye was treated with CXL). The bias towards the male population is consistent with our clinical experience in treating keratoconic patients.^{29–31}

The mean epithelial thickness over an area of 8 mm diameter and central epithelial thickness (where the center is defined as the pupil center) was recorded for each eye from the output of the corneal report, such as shown in Figure 2. In order to estimate variation between the center and the periphery, the average of four points was computed for each eye and reported as Epithelium @ Periphery (Figure 5). Tables 3 and 4 summarize these results and show descriptive statistics.

Table 3 Descriptive statistics for mean (over an area of 8 mm diameter), center, and peripheral epithelium thickness measurements per each study group

Group	Epithelium mean				Epithelium @ pupil center				Epithelium @ periphery			
	Average	SD	Min	Max	Average	SD	Min	Max	Average	SD	Min	Max
Control	50.9	3.7	43	58	52.3	4.9	42	60	49.6	3.1	43	58.25
KCN – not treated	51.9	3.3	45	57	55.1	3.7	46	60	49.8	3.7	43	55
KCN – CXL treated	50.2	3.8	39	57	52.0	5.6	37	60	48.8	3.7	41	58.75

Note: All units μm .
Abbreviations: CXL, crosslinking; KCN, keratoconus; SD, standard deviation.

Table 4 Descriptive statistics performed on the epithelial thickness measurements among the three groups

Mean epithelium	Central epithelium	Peripheral epithelium
t-test: results (the probability of this result, assuming the null hypothesis)		
Control – KCN		
0.17	0.0026	0.69
Control – CXL treated		
0.20	0.93	0.28
KCN – CXL treated		
0.89	0.0026	0.16
three-paired ANOVA		
0.084	0.005	0.28

Abbreviations: ANOVA, ANalysis of Variance; CXL, crosslinking.

Discussion

Epithelium imaging – precision and accuracy

It is evident from our results in Table 2 that, even when acquisition is carefully carried out and all indicators for a successful mapping exist, there is a $\pm 3\text{--}4\ \mu\text{m}$ uncertainty on both corneal and epithelial thickness measurements. The latter is true not only on the nasal, temporal, superior, and inferior points which we examined, but also on the pupil center. While this figure might only be $\pm 0.7\%$ of the corresponding corneal thickness, it corresponds to a 5%–8% uncertainty for the corresponding epithelial thickness.

Our results indicate that there was a statistically significant correlation between central corneal thickness and central epithelium thickness ($R = 0.554$), as measured for the same patient for the same corneal point with different meridian B-scans selection (Figure 3). However, this correlation was not very strong, suggesting that the epithelium does not necessarily follow equally proportional thickness increments as

central corneal thickness. More than 30% of the total sample size was responsible for this correlation.

Regarding accuracy, the comparison of the same eye pachymetry measurements subjected to both AS OCT and Pentacam HR system revealed that there was at least a $10\ \mu\text{m}$ difference between HF UBM and OCT, and a few microns difference between HF UBM and the Pentacam HR. The corneal thickness accuracy, as expressed by the paired correlations between HF UBM, AS OCT, and Pentacam HR, has been studied extensively by our group and has been submitted for publication.³¹

Considering that during the specific acquisition particular care was taken to produce well-centered scans, and the patient was well-educated on the system (ie, the specific case almost fits the description of a best case), we will estimate in all of our following results that the HF UBM epithelium thickness readings have a $\pm 10\%$ or $\pm 5\ \mu\text{m}$ uncertainty. For the rest of our study, we will accept these figures as representative of all reported epithelium thickness measurements.

Epithelium imaging – control group

We observed from the results in Table 3 that average mean corneal epithelial thickness for the control population was $50.9 \pm 3.7\ \mu\text{m}$ (range $43\text{--}58\ \mu\text{m}$). This is in agreement with previously reported values in pertinent publications, which range from $48 \pm 5\ \mu\text{m}$ ³⁴ to $59.9 \pm 5.9\ \mu\text{m}$.^{3,32–35}

In this group of control patients, the epithelium was slightly thicker at the pupil center by an average of $1.3\ \mu\text{m}$ ($52.3 \pm 4.9\ \mu\text{m}$, range $42\text{--}60\ \mu\text{m}$), when compared to the mean thickness. Mean thickness was computed by a small contribution of the area over the pupil center (ie, the thicker part of the epithelium) and by a larger contribution of the peripheral area (where the epithelium is thinner). Therefore, it is no

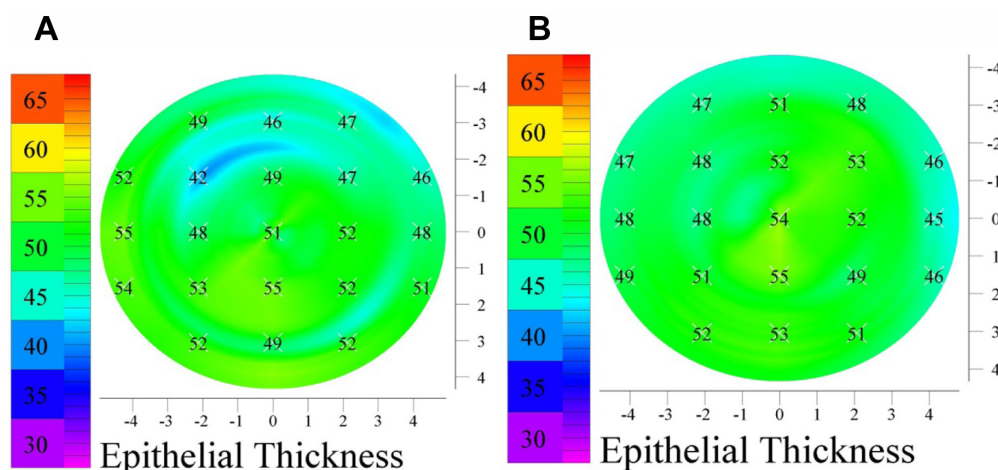


Figure 6 Epithelial thickness maps of the same (control) patient, same eye, as produced by two consecutive acquisitions. Both maps demonstrate a thicker epithelium over the pupil center. Different acquisitions (**A** and **B**) of the same eye may produce epithelium maps which may vary by an estimated $\pm 4\ \mu\text{m}$.

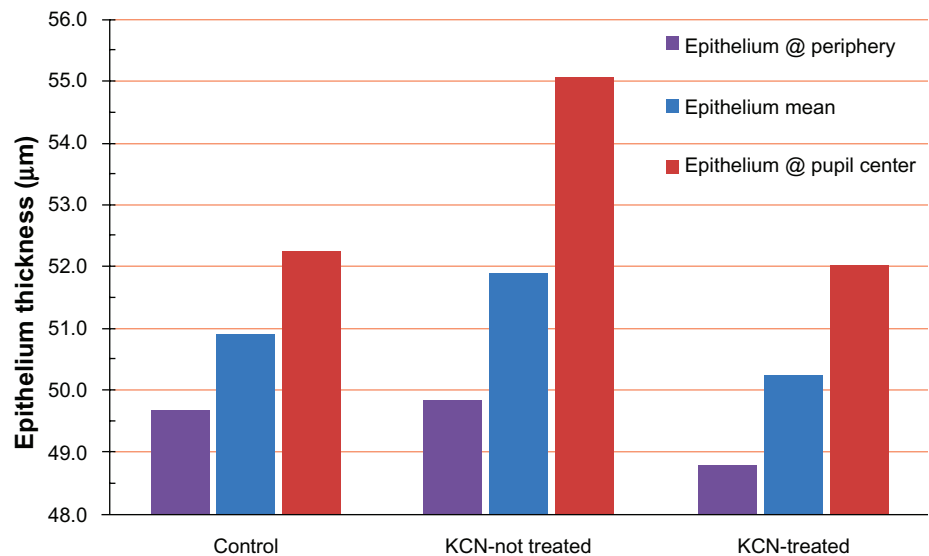


Figure 7 Epithelium thickness across the three study groups, at the periphery, mean, and pupil center.
Abbreviation: KCN, keratoconus.

surprise that while the epithelial center was, on average, thicker by only 1.3 μm compared to the mean, on several occasions it was thicker compared to the nasal, temporal, inferior, or superior points by up to 10 μm . This conclusion is also supported by the fact that the periphery epithelium thickness value of 49.7 μm was closer to the mean (50.9 μm) than to the pupil center (52.3 μm).

We note that the standard deviation of the measurements ($\pm 3\text{--}4\text{ }\mu\text{m}$) is comparable to the accuracy and precision of the

instrument, as established by our investigation, and thus epithelial thickness variations of $\pm 4\text{--}4\text{ }\mu\text{m}$, as it is the case, might be observed differently even on the same eye. An example of a control patient who demonstrated a thicker epithelium at the pupil center is shown in Figure 6. In one instance the central epithelium was elevated by 9 μm (51 μm –42 μm), while in a subsequent examination of the same eye, the difference between the same points was recorded as only 6 μm (54 μm –48 μm).

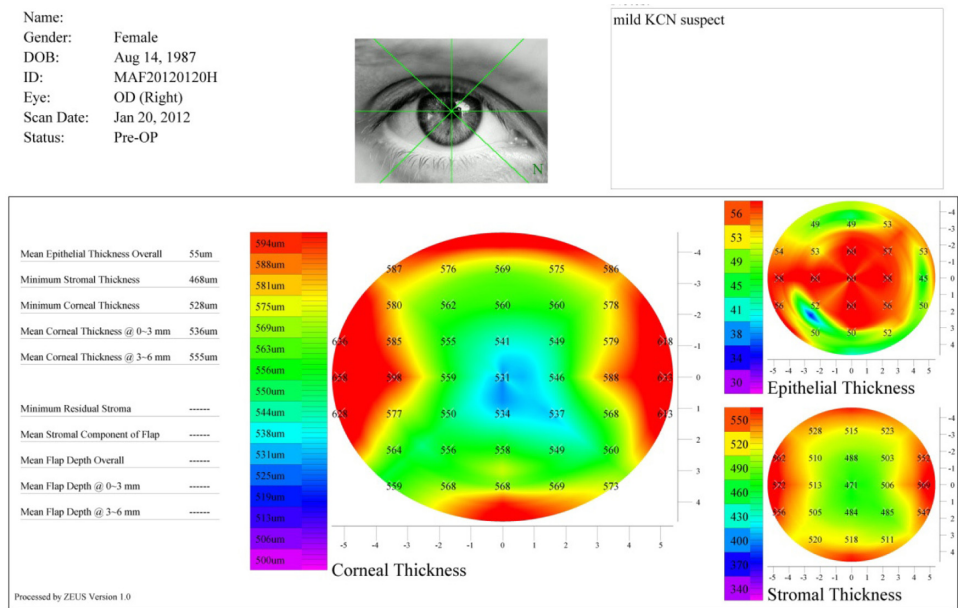


Figure 8 Corneal and epithelial thickness maps of a KCN patient.
Note: A significantly thicker epithelium over the pupil center is observed.
Abbreviation: KCN, keratoconus.

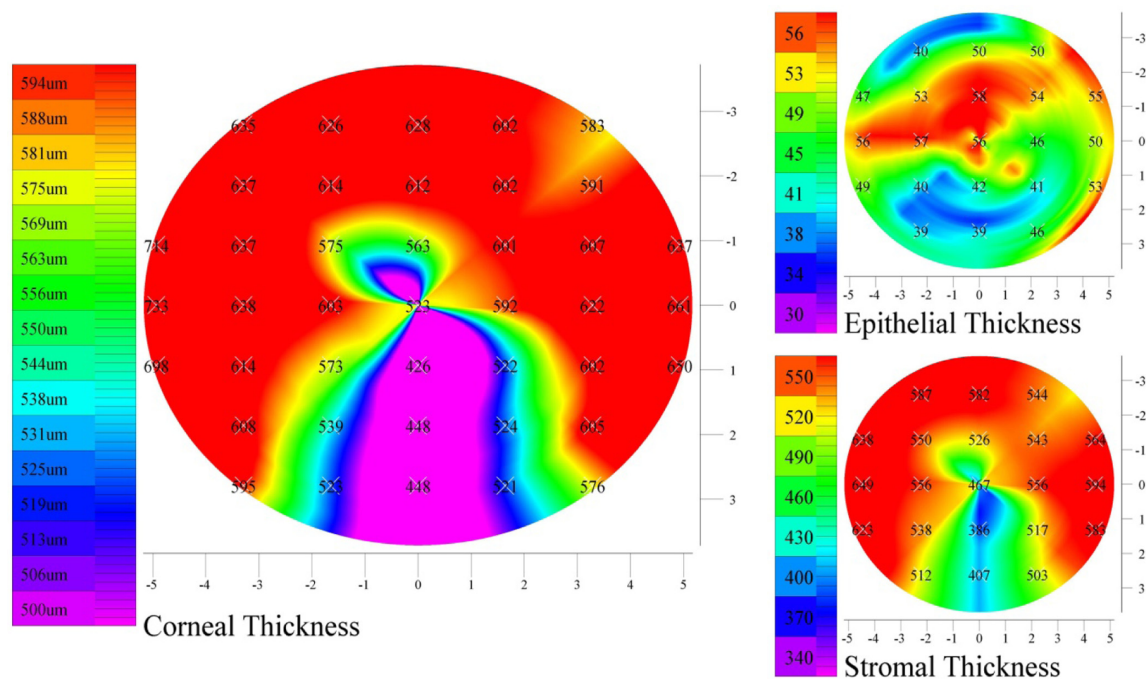


Figure 9 Example of localized thin epithelium (lower segment), over an area of a significantly thinner stroma.

Epithelium imaging – untreated KCN group

The group of untreated KCN patients showed an overall thickening, pronounced at the pupil center. Results over the whole KCN group indicated that on average, the epithelium at the pupil center was 3.1 μm thicker than the mean epithelial thickness (over the entire cornea) (Figure 7). Simultaneously, the epithelium at the periphery was on average $-2.1 \mu\text{m}$ thinner compared to the epithelium mean, and $-5.2 \mu\text{m}$ thinner compared to the central epithelium.

The statistical significance of overall epithelial thickness was supported by descriptive statistics (run by both Origin Lab and SPSS, shown in Table 4.). The three-paired ANOVA test indicated $P = 0.084$ for the mean epithelium values,

0.28 for the epithelium at the periphery, and 0.004 for the epithelium thickness at the pupil center. Furthermore, the two-tailed t -test indicated statistical significance ($P = 0.002$) for the central epithelium between the control and the KCN group, as well as between the CXL-treated KCN and the untreated KCN group ($P = 0.0008$). This was in contrast to the null statistical insignificance ($P = 0.9$) between the control and the CXL-treated groups, further supporting our theory.

We encountered many examples such as shown in Figure 8. It is noteworthy that there is a small area (located temporally-inferiorly), where the epithelium is much thinner. Although not reported on the map, the color scale helps us to estimate that the epithelium over an ectatic area in another example (Figures 9,10A and B) was approximately 35 μm ,

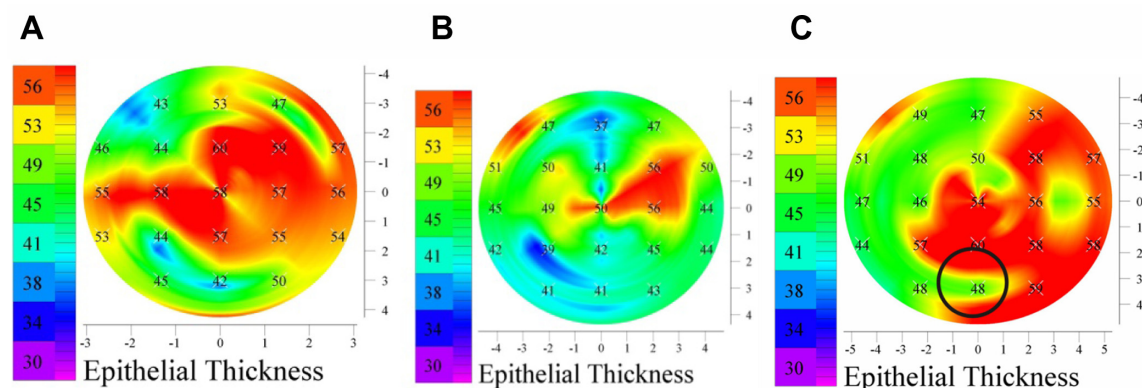


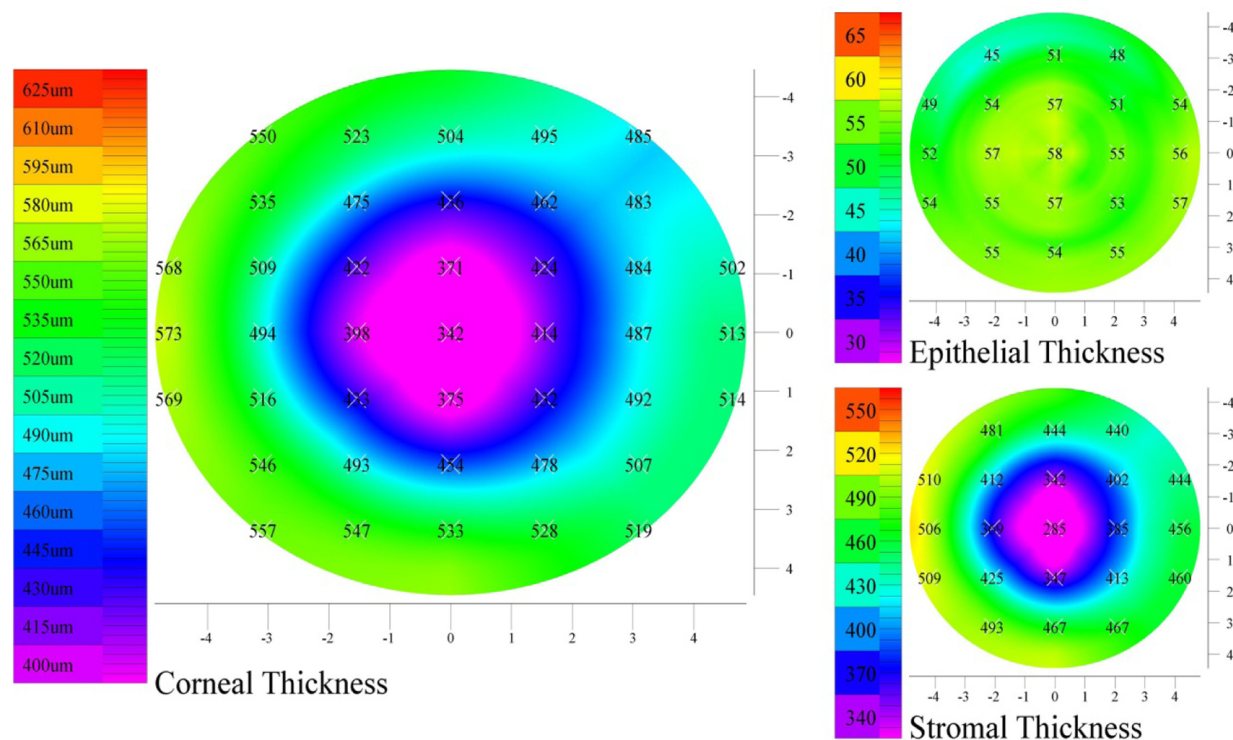
Figure 10 Examples of localized thinner epithelium over protruding corneas. (A and B) KCN patients, (C) a PMD patient.

Abbreviations: KCN, keratoconus; PMD, pellucid marginal degeneration.

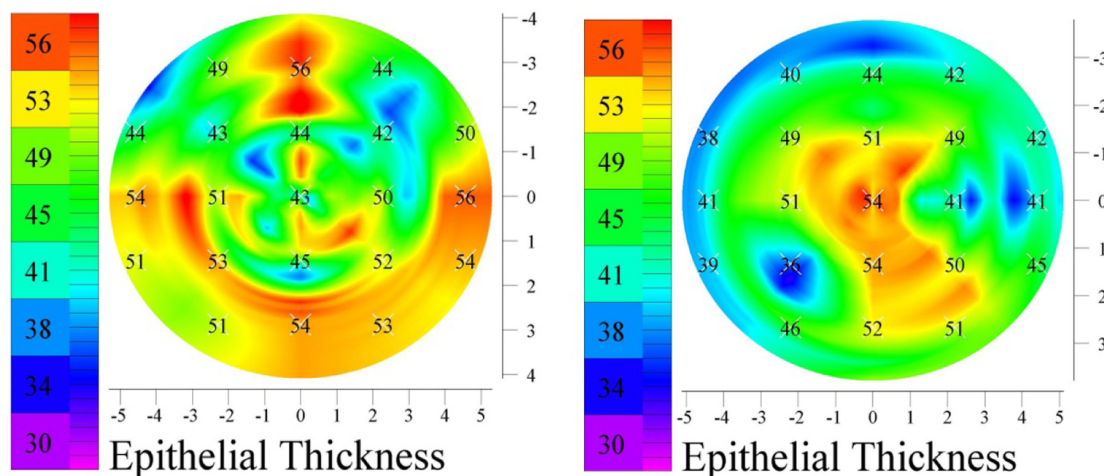
Table 5 Mean, center, and peripheral epithelium thickness, as examined separately for the five younger and the five elder patients from the KCN group

	Age (years)	Epi mean	Epi center	Epi peripheral 4 mm	Age (years)	Epi mean	Epi center	Epi 4 mm
Average	20.9	52.0	55.9	49.7	33.1	51.4	53.4	49.7
Max		57.0	60.0	55.0		55	58	55.00
Min		48	48	44		46	46	43
SD	3.5	3.1	3.8	3.2	3.8	3.6	3.5	4.2

Abbreviations: Epi, epithelium thickness; SD, standard deviation.

**Figure 11** Examples of very smooth epithelium of a patient subjected to CXL.

Abbreviation: CXL, crosslinking.

**Figure 12** Examples of epithelium (patients subjected to CXL and partial topography guided PRK) demonstrating localized variations.

Abbreviations: CXL, crosslinking; PRK, photorefractive keratectomy.

while at the center was almost 60 μm . This is the area of the corneal protrusion, as we can observe from the thinner cornea. In a striking resemblance, the epithelium demonstrated similar characteristics in a pellucid marginal degeneration patient, ie, an area of thin epithelium over the corneal protrusion (Figure 10C).

We believe that the overall thicker epithelium in KCN patients is a result of a reactive process; the epithelium may thicken in less “rigid” corneas due to being more susceptible to mechanical variations produced by one or a combination of the factors below:

1. intraocular pressure variations
2. eye rubbing
3. heart driven blood pulse, translating in a pulsation on the cornea (personal communication: John Marshall, PhD)
4. blinking mechanism.

To further investigate this hypothesis, and considering that keratoconic untreated corneas may become more biomechanically stable with advancing age, we separately examined the five younger (age 20.9 ± 3.5 years) and the five elder (age 33.1 ± 3.8 years) patients from the untreated KCN group.

The results indicate that while the periphery epithelium was identical, compared to the elder group, the average mean epithelium thickness was larger in the younger group by a small margin ($+0.6 \mu\text{m}$) and the central epithelium was statistically thicker ($+2.5 \mu\text{m}$) (Table 5). In other words, the elder group had on average a smoother and slightly thinner epithelium than the younger group.

The CXL treated KCN patients had epithelium thickness distributions that were similar to the control group, rather than the keratoconic group. While in some instances the epithelium was quite normal (Figure 11), most often the epithelium map presented local variations (Figure 12). This particular finding further supports our novel theory of “reactive” epithelial hyperplasia in biomechanically unstable corneas. It appears that in biomechanically stabilized irregular corneas the epithelium becomes “nonreactive” and conforms to more normal thickness, despite the highly irregular underlying stroma contour.

Conclusions

In our study, an overall thicker epithelium with large variations was observed in untreated KCN patients. This is in contrast to previously published work and current understanding. On many occasions the epithelium was significantly thinner over areas of corneal ectasia, in agreement with previous observations.

However, patients subjected to CXL treatment did not show a statistically significant trend towards a thicker “reactive” epithelium, supporting our hypothesis of epithelial hyperplasia in biomechanically unstable corneas.

We feel this may be a significant new finding. In an era when most AS OCT devices will soon be able to offer detailed and accurate cornea epithelial maps, this theory may provide a very sensitive, pre-ectasia clinical parameter in corneas that have become biomechanically unstable. This “reactive” epithelial hypertrophy may precede any of the standard topographic or tomographic cornea findings. For example, “suspect” corneas due to thinner structure, high astigmatism, or even sanguine relation to a known KCN patient may be differentiated in regard to their ectasia potential based on the average cornea epithelial thickness.

The “normalization” of average epithelial thickness in long term follow-up of CXL treated ectasia cases further supports this theory. Further studies are needed to validate these results.

Disclosure

Dr Aslanides is a consultant of Artemis II.

References

1. Simon G, Ren Q, Kervick GN, Parel JM. Optics of the corneal epithelium. *Refract Corneal Surg.* 1993;9(1):42–50.
2. Reinstein DZ, Archer TJ, Gobbe M, Silverman RH, Coleman DJ. Epithelial thickness in the normal cornea: three-dimensional display with very high frequency ultrasound. *J Refract Surg.* 2008;24(6):571–581.
3. Reinstein DZ, Archer T, Gobbe M. Stability of LASIK in corneas with forme fruste or suspect keratoconus, where keratoconus was excluded by epithelial thickness mapping. Presented at: *American Academy of Ophthalmology Annual Meeting*. November 9, 2008; Atlanta, GA.
4. Wang J, Fonn D, Simpson TL, Sorbara L, Kort R, Jones L. Topographical thickness of the epithelium and total cornea after overnight wear of reverse-geometry rigid contact lenses for myopia reduction. *Invest Ophthalmol Vis Sci.* 2003;44:4742–4746.
5. Ladage PM, Yamamoto K, Ren DH, et al. Effects of rigid and soft contact lens daily wear on corneal epithelium, tear lactate dehydrogenase, and bacterial binding to exfoliated epithelial cells. *Ophthalmology.* 2001;108:1279–1288.
6. Holden BA, Stephenson A, Stretton S, et al. Superior epithelial arcuate lesions with soft contact lens wear. *Optom Vis Sci.* 2001;78(1):9–12.
7. Larsson LI, Bourne WM, Pach JM. Structure and function of the corneal endothelium in diabetes mellitus type I and type II. *Arch Ophthalmol.* 1996;114:9–14.
8. Shenoy R, Khandekar R, Bialasiewicz A, Al Muniri A. Corneal endothelium in patients with diabetes mellitus: a historical cohort study. *Eur J Ophthalmol.* 2009;19(3):369–375.
9. Haque S, Simpson T, Jones L. Corneal and epithelial thickness in keratoconus: a comparison of ultrasonic pachymetry, Orbscan II, and optical coherence tomography. *J Refract Surg.* 2006;22(5):486–493.
10. Li Y, Tan O, Huang D. Normal and keratoconic corneal epithelial thickness mapping using Fourier-domain optical coherence tomography. *Proc SPIE.* 2011;7965, 796508; doi:10.1117/12.878567.
11. Feng Y, Simpson TL. Comparison of human central cornea and limbus in vivo using optical coherence tomography. *Optom Vis Sci.* 2005;82:416–419.

12. Eckard A, Stave J, Guthoff RF. In vivo investigations of the corneal epithelium with the confocal Rostock Laser Scanning Microscope (RLSM). *Cornea*. 2006;25(2):127–131.
13. Møller-Pedersen T, Vogel M, Li HF, Petroll WM, Cavanagh HD, Jester JV. Quantification of stromal thinning, epithelial thickness, and corneal haze after photorefractive keratectomy using in vivo confocal microscopy. *Ophthalmology*. 1997;104:360–368.
14. Pérez JG, Méjome JM, Jalbert I, Sweeney DF, Erickson P. Corneal epithelial thinning profile induced by long-term wear of hydrogel lenses. *Cornea*. 2003;22:304–307.
15. Li HF, Petroll WM, Møller-Pedersen T, Maurer JK, Cavanagh HD, Jester JV. Epithelial and corneal thickness measurements by in vivo confocal microscopy through focusing (CMTF). *Curr Eye Res*. 1997;16:214–221.
16. Chen TC, Cense B, Pierce MC, et al. Spectral domain optical coherence tomography: ultra-high speed, ultra-high resolution ophthalmic imaging. *Arch Ophthalmol*. 2005;123(12):1715–1720.
17. Grewal DS, Brar GS, Jain R, Grewal SPS. Comparison of Scheimpflug imaging and spectral domain anterior segment optical coherence tomography for detection of narrow anterior chamber angles. *Eye*. 2011;25:603–611.
18. Wang J, Fonn D, Simpson TL, Jones L. The measurement of corneal epithelial thickness in response to hypoxia using optical coherence tomography. *Am J Ophthalmol*. 2002;133(3):315–319.
19. Sin S, Simpson TL. The repeatability of corneal and corneal epithelial thickness measurements using optical coherence tomography. *Optom Vis Sci*. 2006;83(6):360–365.
20. Prakasam RK, Schwiede M, Hütz WW, Guthoff RF, Stachs O. Corneal responses to eye rubbing with spectral domain optical coherence tomography. *Curr Eye Res*. 2012;37(1):25–32.
21. Reinsteinst DZ, Silverman RH, Coleman DJ. High-frequency ultrasound measurement of the thickness of the corneal epithelium. *Refract Corneal Surg*. 1993;9(5):385–387.
22. Reinsteinst DZ, Silverman RH, Trokel SL, Coleman DJ. Corneal pachymetric topography. *Ophthalmology*. 1994;101(3):432–438.
23. Denoyer A, Ossant F, Arbeille B, et al. Very-high-frequency ultrasound corneal imaging as a new tool for early diagnosis of ocular surface toxicity in rabbits treated with a preserved glaucoma drug. *Ophthalmic Res*. 2008;40:298–308.
24. Mundt GH, Hughes WF. Ultrasonics in ocular diagnosis. *Am J Ophthalmol*. 1956;42:488–498.
25. Baum G, Greenwood I. The application of ultrasonic locating techniques to ophthalmology. II. Ultrasonic slit-lamp in the ultrasonic visualization of soft tissues. *Arch Ophthalmol*. 1958;60:263–279.
26. Pavlin CJ, Harasiewicz K, Sherar MD, Foster FS. Clinical use of ultrasound biomicroscopy. *Ophthalmology*. 1991;98:287–295.
27. Pavlin CJ, Sherar MD, Foster FS. Subsurface ultrasound microscopic imaging of the intact eye. *Ophthalmology*. 1990;97:244–250.
28. Reinsteinst DZ, Silverman RH, Raevsky T, et al. Arc-scanning very high-frequency digital ultrasound for 3D pachymetric mapping of the corneal epithelium and stroma in laser in situ keratomileusis. *J Refract Surg*. 2000;16:414–430.
29. Kanellopoulos AJ. Comparison of sequential vs same-day simultaneous collagen cross-linking and topography-guided PRK for treatment of keratoconus. *J Refract Surg*. 2009;25(9):S812–S818.
30. Kanellopoulos AJ. Long term results of a prospective randomized bilateral eye comparison trial of higher fluence, shorter duration ultraviolet A radiation, and riboflavin collagen cross linking for progressive keratoconus. *Clin Ophthalmol*. 2012;6:97–101.
31. Kanellopoulos AJ, Aslanides IM, Asimellis G. Clinical correlation between corneal pachymetry measurements by Scheimpflug-image cornea tomography (Oculus II-Pentacam HR), anterior segment optical coherence tomography and high-frequency scanning ultrasound biomicroscopy. (submitted Jan 2012).
32. Wang J, Thomas J, Cox I, Rollins A. Noncontact measurements of central corneal epithelial and flap thickness after laser in situ keratomileusis. *Invest Ophthalmol Vis Sci*. 2004;45:1812–1816.
33. Wirbelauer C, Pham DT. Monitoring corneal structures with slit-lamp-adapted optical coherence tomography in laser in situ keratomileusis. *J Cataract Refract Surg*. 2004;30:1851–1860.
34. Haque S, Fonn D, Simpson T, Jones L. Corneal and epithelial thickness changes after 4 weeks of overnight corneal refractive therapy lens wear, measured with optical coherence tomography. *Eye Contact Lens*. 2004;30:189–193.
35. Møller-Pedersen T, Li HF, Petroll WM, Cavanagh HD, Jester JV. Confocal microscopic characterization of wound repair after photorefractive keratectomy. *Invest Ophthalmol Vis Sci*. 1998;39:487–501.

Clinical Ophthalmology

Publish your work in this journal

Clinical Ophthalmology is an international, peer-reviewed journal covering all subspecialties within ophthalmology. Key topics include: Optometry; Visual science; Pharmacology and drug therapy in eye diseases; Basic Sciences; Primary and Secondary eye care; Patient Safety and Quality of Care Improvements. This journal is indexed on

Submit your manuscript here: <http://www.dovepress.com/clinical-ophthalmology-journal>

Dovepress

PubMed Central and CAS, and is the official journal of The Society of Clinical Ophthalmology (SCO). The manuscript management system is completely online and includes a very quick and fair peer-review system, which is all easy to use. Visit <http://www.dovepress.com/testimonials.php> to read real quotes from published authors.